

**Jet rates in deep inelastic scattering: wherefrom comes the sensitivity to  $\alpha_s$ ?***Jiří Chýla and Jiří Rameš*Institute of Physics, Academy of Sciences of the Czech Republic, Prague <sup>1</sup>**Abstract**

For theoretically consistent determination of  $\alpha_s$  from jet rates in deep inelastic scattering the dependence on  $\alpha_s$  of parton distribution functions is in principle as important as that of hard scattering cross-sections. For the kinematical region accessible at HERA we investigate in detail numerical importance of these two sources of the  $\alpha_s$  dependence of jet rates.

**1 Introduction**

One of the problems of quantitative determination of the running of  $\alpha_s$  is related to the fact that it usually requires combining results of different experiments in different kinematical regions. Recently the H1 [1] and ZEUS [2] Collaborations have reported evidence for the running of  $\alpha_s(\mu)$  obtained from the measurement of jet rates in deep inelastic scattering (DIS) via the quantity

$$R_{2+1}(Q^2) \equiv \frac{\sigma_{2+1}(Q^2)}{\sigma_{1+1}(Q^2) + \sigma_{2+1}(Q^2)}, \quad (1)$$

where  $\sigma_{k+1}$  denotes the cross-section for the production of  $k$  hard and one proton remnant jets. There are now several NLO Monte-Carlo generators [3, 4, 5], suitable for analyses of jet production in DIS. In this paper we shall concentrate on the H1 analysis [1] which, using PROJET 4.1 [3] with the JADE jet algorithm and  $y_c = 0.02$ , obtained the following result for  $\alpha_s(M_Z, \overline{\text{MS}})$

$$\alpha_s(M_Z, \overline{\text{MS}}) = 0.123 \pm 0.012(\text{stat.}) \pm 0.008(\text{syst.}). \quad (2)$$

In JADE cluster algorithm, the jet resolution parameter  $y_c$  is defined as  $y_c = (p_i + p_j)^2/W^2$ , where  $p_i, p_j$  are parton momenta and  $W^2 = Q^2(1-x)/x$  stands for the square of the  $\gamma p$  CMS energy. The result (2) has been extracted from the  $Q^2$ -dependence of  $R_{2+1}(Q^2)$ , displayed in Fig. 2 of [1], using only the two highest  $Q^2$  data points. Within the error bars the value (2) is consistent with the world average, but its accuracy is insufficient to draw any firmer conclusions. In the procedure adopted in [1]  $\alpha_s(\mu, \overline{\text{MS}})$  (or, equivalently,  $\Lambda_{\overline{\text{MS}}}$ ) was considered as a free parameter in the hard scattering cross-sections, but not in the parton distribution functions (PDF), for which the MRSH set was used. However, as each set of PDF has a particular value of  $\Lambda_{\overline{\text{MS}}}$  built in, one must check for the consistency between this input  $\Lambda_{\overline{\text{MS}}}$  and the output one, obtained from comparison of (1) with data. Clearly, in a consistent determination of  $\alpha_s$ ,  $\Lambda_{\overline{\text{MS}}}$  must be varied simultaneously in PDF and parton level hard scattering cross-sections. In practical applications to physical quantities involving beside the hard scattering cross-sections also parton distribution and/or fragmentation functions it is often useful to know wherefrom comes most of the sensitivity to  $\alpha_s$ . The purpose of our paper is to investigate this question in detail for the jet rates (1).

---

<sup>1</sup>e-mail: chyla@fzu.cz, rames@fzu.cz

Throughout this paper we stay in the conventional  $\overline{\text{MS}}$  renormalization scheme (RS) of the couplant  $a \equiv \alpha_s(\mu)/\pi$  and omit therefore the specification “ $\overline{\text{MS}}$ ” in  $\Lambda_{\overline{\text{MS}}}$  as well as in  $\alpha_s(\mu, \overline{\text{MS}})$ . The jet cross-sections  $\sigma_{k+1}$  in (1) are given as convolutions

$$\sigma_{k+1}(Q^2, y_c, \Lambda) \equiv \sum_i \int_0^1 dx f_i(x, M, \Lambda) C_{k+1,i}(Q, M, x, y_c, \Lambda) \quad (3)$$

of the parton level cross-sections  $C_{k+1,i}$  and PDF  $f_i(x, M)$ , evaluated at the factorization scale  $M$ . The sum runs over all parton species  $i$ . In perturbative QCD  $C_{k+1,i}$  are given as expansions in the couplant  $a(\mu/\Lambda)$ , taken at the hard scattering scattering scale  $^2 \mu$ . To the NLO we have

$$C_{2+1,i}(Q, M, x, y_c, \Lambda) = a(\mu/\Lambda) \left[ c_{2+1,i}^{(1)}(Q^2, x, y_c) + a(\mu/\Lambda) c_{2+1,i}^{(2)}(Q, M, x, y_c) \right],$$

$$C_{1+1,i}(Q, M, x, y_c, \Lambda) = c_{1+1,i}^{(0)}(Q, x) + a(\mu/\Lambda) c_{1+1,i}^{(1)}(Q, M, x, y_c). \quad (4)$$

In standard global analyses of hard scattering processes [7, 8, 9],  $\Lambda$  is fitted together with a set of parameters  $a_i^{(j)}$ , describing distribution functions  $p^{(j)}(x, M)$  of parton species  $j$  at some initial scale  $M_0$ , usually in the form

$$p^{(j)}(x, M_0) = a_0^{(j)} x^{a_1^{(j)}} (1-x)^{a_2^{(j)}} \left( 1 + a_3^{(j)} \sqrt{x} + a_4^{(j)} x + a_5^{(j)} x^{3/2} \right). \quad (5)$$

Writing the derivative  $d\sigma_{2+1}/d \ln \Lambda$  as

$$\begin{aligned} \frac{d\sigma_{2+1}(Q^2, \Lambda)}{d \ln \Lambda} = & \sum_i \int_0^1 dx \left[ \frac{df_i(x, M, \Lambda)}{d \ln \Lambda} a(M) c_{2+1,i}^{(1)}(x) + f_i(x, M, \Lambda) c_{2+1,i}^{(1)}(x) \frac{da(M)}{d \ln \Lambda} \right] = \\ & a(M) \sum_{ij} \int_0^1 dx \left[ - \int_0^1 \frac{dy}{y} f_j(y, M, \Lambda) P_{ij}^{(0)}(z) a(M) c_{2+1,i}^{(1)}(x) + \right. \\ & \left. b f_i(x, M, \Lambda) a(M) c_{2+1,i}^{(1)}(x) \right], \end{aligned} \quad (6)$$

where  $z \equiv x/y$  and  $P_{ij}^{(0)}(z)$  are the LO branching functions  $^3$ , we see that the leading order term of  $d\sigma_{2+1}/d \ln \Lambda$  gets contributions from the variation of  $\Lambda$  in both the PDF  $f_i$  and hard scattering cross-sections  $C_{2+1,i}$ . The two terms in the brackets of (6) are of the same order and their relative importance thus is basically a LO effect.

For the quantity  $R_{2+1}(Q^2)$  the situation is less obvious. PDF appear in both the numerator and denominator of (1) and so some cancellations might occur, while the hard scattering cross-sections start as  $O(a)$  for  $C_{2+1,i}$  and as  $O(1)$  for  $C_{1+1,i}$ . Nevertheless a detailed analysis [10] shows that also for the ratio  $R_{2+1}$  varying  $\Lambda$  in PDF generates terms which are of the same order as those resulting from the variation of  $\Lambda$  in the hard scattering cross-sections  $C_{k+1,i}$ .

## 2 Parton distribution functions for arbitrary $\Lambda$

To assess the potential of (1) for a precise determination of  $\alpha_s$  we wish to separate the question of its sensitivity to  $\alpha_s$  from the sensitivity to parameters describing the initial condition on the PDF.

<sup>2</sup>Although in general  $\mu \neq M$ , we shall follow the usual practice and set  $\mu = M$ .

<sup>3</sup>In (6) we have for brevity suppressed the dependence of  $c_{2+1,i}^{(1)}$  on  $y_c$  and written  $a(M/\Lambda)$  simply as  $a(M)$ .

Moreover, in order to investigate the numerical importance of varying  $\Lambda$  in PDF we have to know what to do with the parameters  $M_0, a_i^{(j)}$  in (5) when  $\Lambda$  is varied. We cannot keep them fixed as this would contradict the idea of factorization. To see why, let us first consider the couplant as well as the evolution equation for the nonsinglet quark distribution function  $q_{\text{NS}}(x, M)$ , at the LO. In terms of conventional moments we have

$$\frac{dq_{\text{NS}}(n, M, \Lambda)}{d \ln M} = a(M/\Lambda) q_{\text{NS}}(n, M) P_{\text{NS}}^{(0)}(n), \quad d_n \equiv -P_{\text{NS}}^{(0)}(n)/b, \quad (7)$$

whence

$$q_{\text{NS}}(n, M, \Lambda) = A_n [a(M/\Lambda)]^{d_n}, \quad a(M/\Lambda) = \frac{1}{b \ln(M/\Lambda)}. \quad (8)$$

In the above expressions  $P_{\text{NS}}^{(0)}(n, M)$  are moments of LO nonsinglet branching function and  $A_n$  are unique dimensionless constants, describing the nonperturbative properties of the nucleon, introduced in [11]. Via (8) they determine the asymptotic behavior of  $q_{\text{NS}}(n, M, \Lambda)$  for  $M \rightarrow \infty$  and thus provide alternative way of specifying the initial conditions on the solutions of (7). The separation in (8) of  $q_{\text{NS}}(n, M, \Lambda)$  into two parts – one calculable in perturbation theory and the other incorporating all the nonperturbative effects – is the very essence of the factorization idea. Note that in (8) the dependence on  $\Lambda$  is simply a reflection of its dependence on  $M$ . Knowing the latter, we know the former. Eq. (8) implies that we can write down the equations for the  $\Lambda$ -dependence of PDF which are very similar to standard evolution equations, describing their dependence on the factorization scale  $M$ . The situation is basically the same as for the running couplant  $a(M/\Lambda)$  for which  $da(M/\Lambda)/d \ln \Lambda = -da(M/\Lambda)/d \ln M$ . In the case of PDF the only difference stems from the necessity to properly specify the initial conditions on the solution of (7). For finite initial  $M_0$  (8) implies

$$q_{\text{NS}}(n, M, \Lambda) = q_{\text{NS}}(n, M_0, \Lambda) \left[ \frac{a(M/\Lambda)}{a(M_0/\Lambda)} \right]^{d_n} = q_{\text{NS}}(n, M_0, \Lambda) \exp(-d_n s), \quad (9)$$

where

$$s \equiv \ln \left( \frac{\ln(M/\Lambda)}{\ln(M_0/\Lambda)} \right) \doteq \ln \left( \frac{a(M_0/\Lambda)}{a(M/\Lambda)} \right) \quad (10)$$

is the so called “evolution distance” [9]. The second equality in (10) holds exactly at the leading order and approximately at higher ones. Rewriting (9) again in the form (8)

$$q_{\text{NS}}(n, M, \Lambda) = \left[ \frac{q_{\text{NS}}(n, M_0, \Lambda)}{(a(M_0/\Lambda))^{d_n}} \right] (a(M/\Lambda))^{d_n} \quad (11)$$

we see that the ratio of  $q_{\text{NS}}(n, M_0, \Lambda)$  and  $(a(M_0/\Lambda))^{d_n}$  equals  $A_n$  and must therefore be both  $M_0$  and  $\Lambda$  independent. This, however, is possible only if the initial moments  $q_{\text{NS}}(n, M_0, \Lambda)$  do, as indicated, depend beside  $M_0$  on  $\Lambda$  as well! Note that considering  $q_{\text{NS}}(n, M, \Lambda)$  as a function of  $s$ , formula (11) implies that entire dependence of  $q_{\text{NS}}(n, M, \Lambda)$  on  $\Lambda$  comes solely from the term  $\ln(M/\Lambda) = 1/a(M/\Lambda)$  in (10)! The same happens in the realistic case of coupled quark and gluon evolution equations [12]. If we wish to investigate the dependence of PDF solely on  $\Lambda$ , keeping fixed all other parameters, specifying the initial conditions on PDF, we cannot fix initial conditions at some finite  $M_0$ , (i.e. the parameters  $p^{(j)}(x, M_0)$  in (5)). It is the constants  $A_n$  that must be kept fixed instead! On the other hand, in global analyses, like [7, 8, 9], all parameters, including  $\Lambda$ , are varied simultaneously and fitted to data. In these circumstances it is then not straightforward to determine the sensitivity of a given physical quantity to  $\alpha_s$  itself.

The preceding paragraph also suggests a simple procedure, which makes use of some of the available parameterizations and generalizes them to arbitrary  $\Lambda$ , keeping the constants  $A_n$  fixed. From all the available parameterizations of PDF those given by analytic expressions of the coefficients  $a_i^{(j)}$  on a general factorization scale  $M$  via the variable  $s$  are particularly suitable for this purpose. In our studies we took several of the GRV parameterizations, both LO and NLO ones, defined in [13]. At the LO the recipe for construction of PDF for arbitrary  $\Lambda$  is simple:

- Use any of these parameterizations with fitted value of  $\Lambda_{fit}$ .
- Keep  $\Lambda$  in  $\ln(M_0/\Lambda)$  fixed at the value  $\Lambda_{fit}$ .
- Vary  $\Lambda$  in  $\ln(M/\Lambda)$ .
- Use the original parameterization with the redefined  $s = s(\Lambda)$ .

This construction is exact at the LO. At the NLO the couplant  $a(M/\Lambda)$  is no longer given simply as  $1/\ln(M/\Lambda)$  and consequently the second equality in (10) holds only approximately. This, together with the additional term appearing in the NLO expression for  $q_{NS}(n, M, \Lambda)$

$$q_{NS}(n, M, \Lambda, A_n) = A_n \left[ \frac{a(M/\Lambda)}{1 + ca(M/\Lambda)} \right]^{d_n} (1 + ca(M/\Lambda))^{P_{NS}^{(1)}(n)/bc}, \quad (12)$$

destroy simple dependence of  $q_{NS}$  on  $M, M_0$  and  $\Lambda$  via the variable  $s$ . Using the above recipe for the NLO GRV parameterizations provides therefore merely an approximate solution of our task, but one that is sufficient for the purposes of determining the relative importance of varying  $\Lambda$  in PDF and hard scattering cross-sections as this relative importance is basically a LO effect.

As an illustration of our procedure we plot in Fig. 1, for  $x \geq 10^{-4}$  and two values of  $Q^2$ , the dependence of valence and sea  $u$ -quark and gluon distribution functions on  $\Lambda$ . The curves correspond to the LO GRV parameterization of [13]. We see that this dependence decreases with increasing  $Q^2$ , is most pronounced for the gluon distribution function and almost irrelevant for the valence quark one. These features are qualitatively the same as those obtained in refs. [14, 15], which contain results of global fits performed for several fixed values of  $\Lambda$ . Quantitatively, however, the sensitivity to the variation of  $\Lambda$ , observed in these papers, is markedly weaker than that displayed in Fig. 1. This is due to the fact that our  $\Lambda$ -dependent PDF are not constructed to describe the hard scattering data for all values of  $\Lambda$  (they do so by definition only for  $\Lambda = \Lambda_{fit}$ ) but in order to facilitate studies of the dependence of physical quantities solely on  $\Lambda$ , with the appropriate parameters specifying the initial conditions kept fixed. On the other hand, in global analyses of [14, 15] fitting the data for different values of  $\Lambda$  leads to different values of boundary condition parameters  $a_i^{(j)}$  at  $M_0$ , which partially compensates the variation of  $\Lambda$ .

### 3 Numerical results

All the results reported below were obtained using the PROJET 4.1 generator [3]. It is true that the JADE jet algorithm used in this program has certain theoretical shortcomings, but as the H1 Collaboration used it, we did the same. Although MC generator MEPJET [4] is to be preferred on theoretical grounds, the main features of our results are unlikely to change because the  $\Lambda$ -dependence of  $R_{2+1}$  is basically a LO effect. To quantify the dependence of  $R_{2+1}$  on  $\Lambda$  separately in hard scattering cross-sections and PDF we consider it as a function of  $Q^2, y_c$  and two independent  $\Lambda$ -parameters, denoted as  $\Lambda^{hsc}$  and  $\Lambda^{pdf}$  respectively. The results are then studied as a function of  $\Lambda^{hsc}, \Lambda^{pdf}, Q^2$  and  $y_c$  for

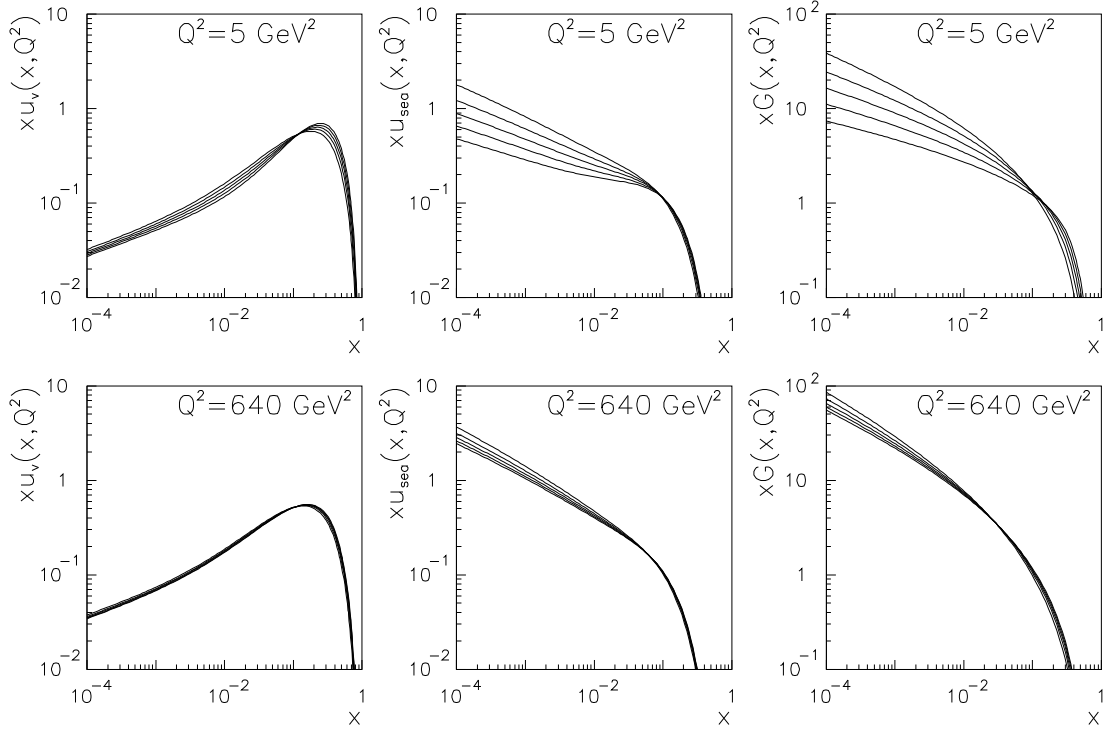


Figure 1: The dependence of  $x u_v(x, Q^2)$ ,  $x u_{\text{sea}}(x, Q^2)$  and  $x G(x, Q^2)$  of the value  $\Lambda^{\text{pdf}}$  according to the recipe described in the text and for two values of  $Q^2$ . At low  $x$ , the curves correspond from above to the values of  $\Lambda^{\text{pdf}}$ , subsequently,  $0.1, 0.2, 0.3, 0.4$  and  $0.5$ .

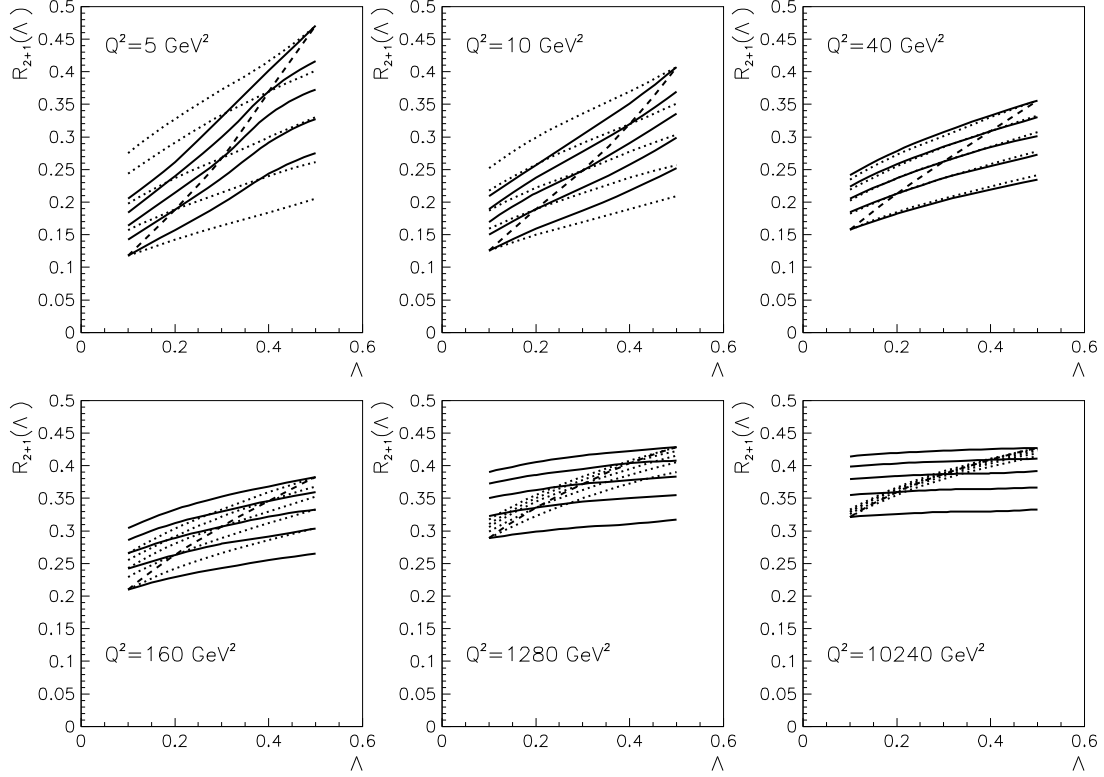


Figure 2: The ratio  $R_{2+1}(Q, y_c, \Lambda^{\text{pdf}}, \Lambda^{\text{hsc}})$  as a function of  $\Lambda^{\text{pdf}}$  for fixed  $\Lambda^{\text{hsc}}$  and a series of  $Q^2$  values (solid lines), or as a function of  $\Lambda^{\text{hsc}}$  for fixed  $\Lambda^{\text{pdf}}$  and the same set of  $Q^2$  values (dotted lines). The dashed lines correspond to simultaneous variation of  $\Lambda^{\text{pdf}} = \Lambda^{\text{hsc}}$ . Solid curves correspond, from below, to fixed  $\Lambda^{\text{hsc}} = 0.1, 0.2, 0.3, 0.4, 0.5$  and the dotted to the same fixed values of  $\Lambda^{\text{pdf}}$ . In all plots  $y_c$  equals 0.01.

- 12 values of  $Q^2$  (equidistant in  $\ln Q^2$ ) between 5 and  $10^4$   $\text{GeV}^2$ ,
- 5 values of  $\Lambda^{\text{pdf}}$  or  $\Lambda^{\text{hsc}}$ , equal to 0.1, 0.2, 0.3, 0.4 and 0.5  $\text{GeV}$ ,
- 3 values of  $y_c = 0.01, 0.02, 0.04$ .

### 3.1 No cuts on jets

First we analyse the case with no cuts on the final state jets and then discuss the changes caused by the imposition of cuts as specified in [1]. Fig. 2 shows a series of plots corresponding to  $y_c = 0.01$  and displaying the dependence of  $R_{2+1}^{\text{NLO}}$  on  $\Lambda^{\text{hsc}}$  for fixed  $\Lambda^{\text{pdf}}$  (dotted curves) or on  $\Lambda^{\text{pdf}}$  for fixed  $\Lambda^{\text{hsc}}$  (solid curves). Each plot corresponds to one of the 6 selected values of  $Q^2$ . We see that for  $Q^2$  below about 40  $\text{GeV}^2$  the solid curves are steeper than the dotted ones, while above 40  $\text{GeV}^2$  the situation is reversed. This means that below 40  $\text{GeV}^2$  varying  $\Lambda$  in PDF is more important than varying it in the hard scattering cross-sections for  $Q^2$ , while the opposite holds above 40

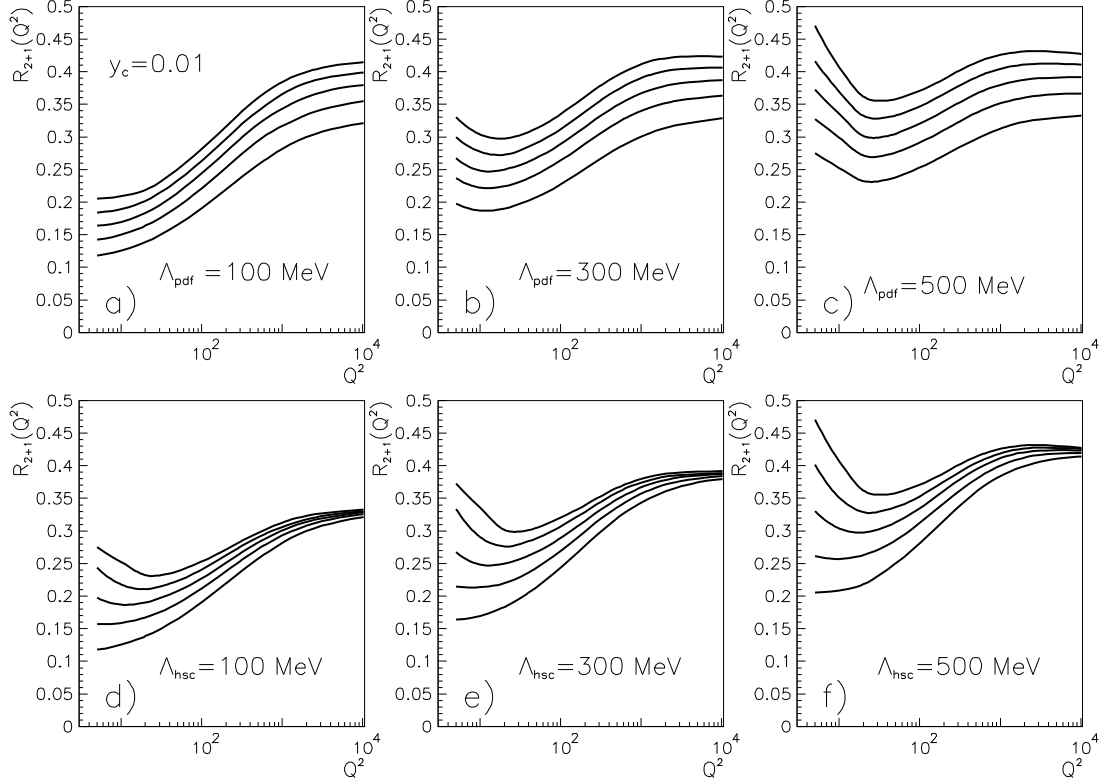


Figure 3: (a–c)  $Q^2$ –dependence of the ratio  $R_{2+1}(Q, y_c, \Lambda^{\text{pdf}}, \Lambda^{\text{hsc}})$  for fixed  $\Lambda^{\text{pdf}} = 0.1, 0.3, 0.5$  GeV and five values of  $\Lambda^{\text{hsc}} = 0.1, 0.2, 0.3, 0.4, 0.5$  GeV. (d–f) The role of  $\Lambda^{\text{pdf}}$  and  $\Lambda^{\text{hsc}}$  is reversed. No cuts were applied in evaluating  $R_{2+1}$  and  $y_c = 0.01$ . In all plots the curves are ordered from below according to increasing  $\Lambda^{\text{hsc}}$  (in a–c) or  $\Lambda^{\text{pdf}}$  (in d–f).

$\text{GeV}^2$ . The same information as in Fig. 2 is displayed in a different manner in Fig. 3, where the  $Q^2$  dependence of  $R_{2+1}$  is plotted for various combinations of  $\Lambda^{\text{pdf}}$  and  $\Lambda^{\text{hsc}}$ . The shape of the curves in Fig. 3 is a result of two opposite effects: as  $Q^2$  increases the phase space available for produced jets increases as well, but at the same time the value of the running  $\alpha_s(Q/\Lambda)$  decreases. At low  $Q^2$ , on the other hand, phase space shrinks, but  $\alpha_s(Q/\Lambda)$  grows.

In Fig. 3 the relative importance of varying  $\Lambda^{\text{pdf}}$  and  $\Lambda^{\text{hsc}}$  is reflected in a bigger spread of the five curves in Figs. 3d)–f) compared to those in Fig. 3a)–c) for  $Q^2 \leq 40 \text{ GeV}^2$  and smaller spread above  $40 \text{ GeV}^2$ . Note also that for fixed  $\Lambda^{\text{pdf}}$  the sensitivity to the variation of  $\Lambda^{\text{hsc}}$  is about the same at all  $Q^2$ . The shape of curves in Fig. 2 suggests that the ratio

$$V(Q^2, y_c, r, s) \equiv \frac{R_{2+1}(Q^2, y_c, \Lambda^{\text{pdf}} = s, \Lambda^{\text{hsc}} = r)}{R_{2+1}(Q^2, y_c, \Lambda^{\text{pdf}} = r, \Lambda^{\text{hsc}} = s)}, \quad (13)$$

is approximately a linear function of  $s$  for any fixed  $Q^2, y_c, r$ . Considered as a function of  $s$  for fixed  $r$ , (13) quantifies the relative importance of varying  $\Lambda$  in PDF and hard scattering cross-sections.

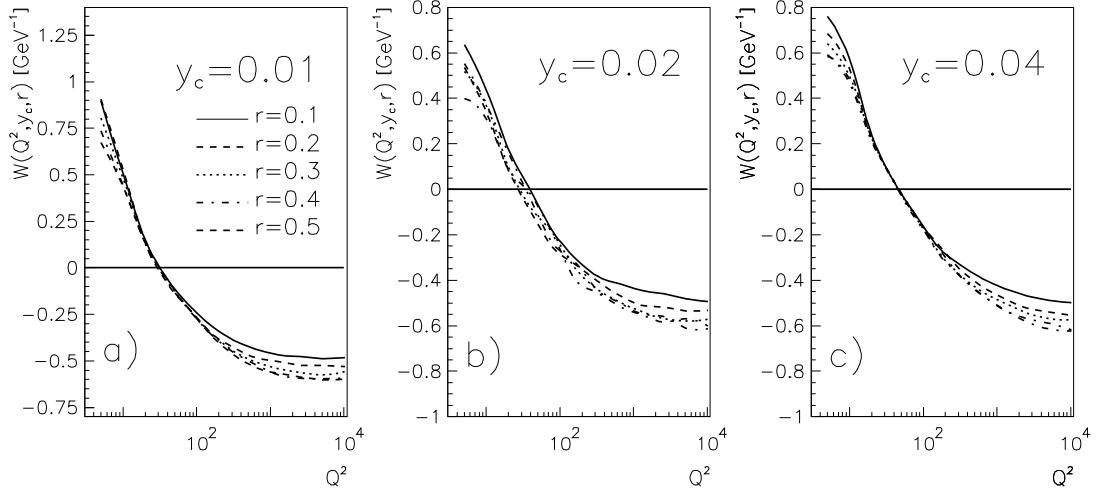


Figure 4: (a–c) The quantity  $W(Q^2, y_c, r)$  as a function of  $Q^2$  for five values of  $r$  (given in GeV) and  $y_c = 0.01, 0.02, 0.04$ . All curves correspond to the case of no cuts.

To summarize the results of Fig. 2 we fitted  $V(Q^2, y_c, r, s)$  by a linear function of  $s$  and defined

$$W(Q^2, y_c, r) \equiv \frac{dV^{fit}(Q^2, y_c, r, s)}{ds}, \quad (14)$$

which, by construction, is  $s$ -independent function of  $Q^2, y_c$  and  $r$ . Positive  $W$  means that the variation of  $\Lambda$  in the PDF is more important than that in the hard scattering cross-sections, while for negative  $W$  the situation is opposite. The  $Q^2$ -dependence of  $W(Q^2, y_c, r)$  is plotted in Fig. 4a–c for three values of  $y_c = 0.01, 0.02, 0.04$  and five values of  $r = 0.1, 0.2, 0.3, 0.4, 0.5$  GeV. In Fig. 5a we compare the  $Q^2$  dependence of  $W(Q^2, y_c, r = 0.2 \text{ GeV})$  for different values of  $y_c = 0.01, 0.02, 0.04$ . Similar plots can be drawn for other values of  $r$  as well. From Figs. 2–5a we conclude that at the NLO:

- For  $Q^2$  below 40 GeV<sup>2</sup> the sensitivity of (1) to  $\Lambda$  comes dominantly from PDF, while above 40 GeV<sup>2</sup> the situation rapidly changes and most of this sensitivity comes from hard scattering cross-section.
- Above  $Q^2 \approx 10^3$  GeV<sup>2</sup> the sensitivity to  $\Lambda$  in PDF becomes negligible.
- The preceding conclusions depend only weakly on  $y_c$ .

At the LO the general features are the same as those displayed in Figs. 2–5a and we therefore merely summarize them in Fig. 5b. Comparing Figs. 5a and 5b we conclude that at the LO the relative importance of varying  $\Lambda^{\text{pdf}}$  with respect to  $\Lambda^{\text{hsc}}$  is bigger than at the NLO.



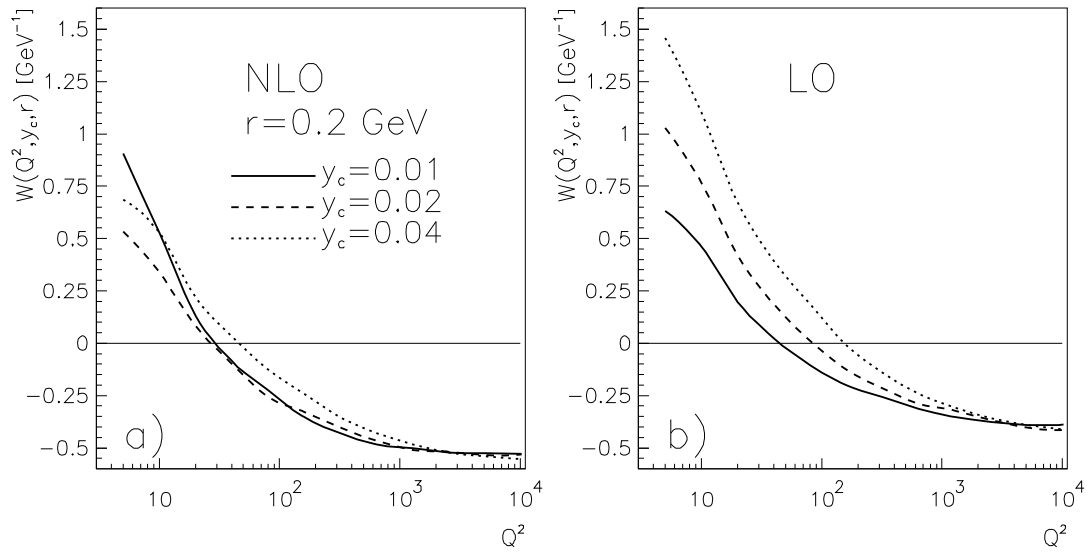


Figure 5: The  $Q^2$ -dependence of  $W(Q^2, y_c, r = 0.2)$  for three different values of  $y_c$  at the NLO (a) and LO (b). All curves correspond to the case of no cuts.

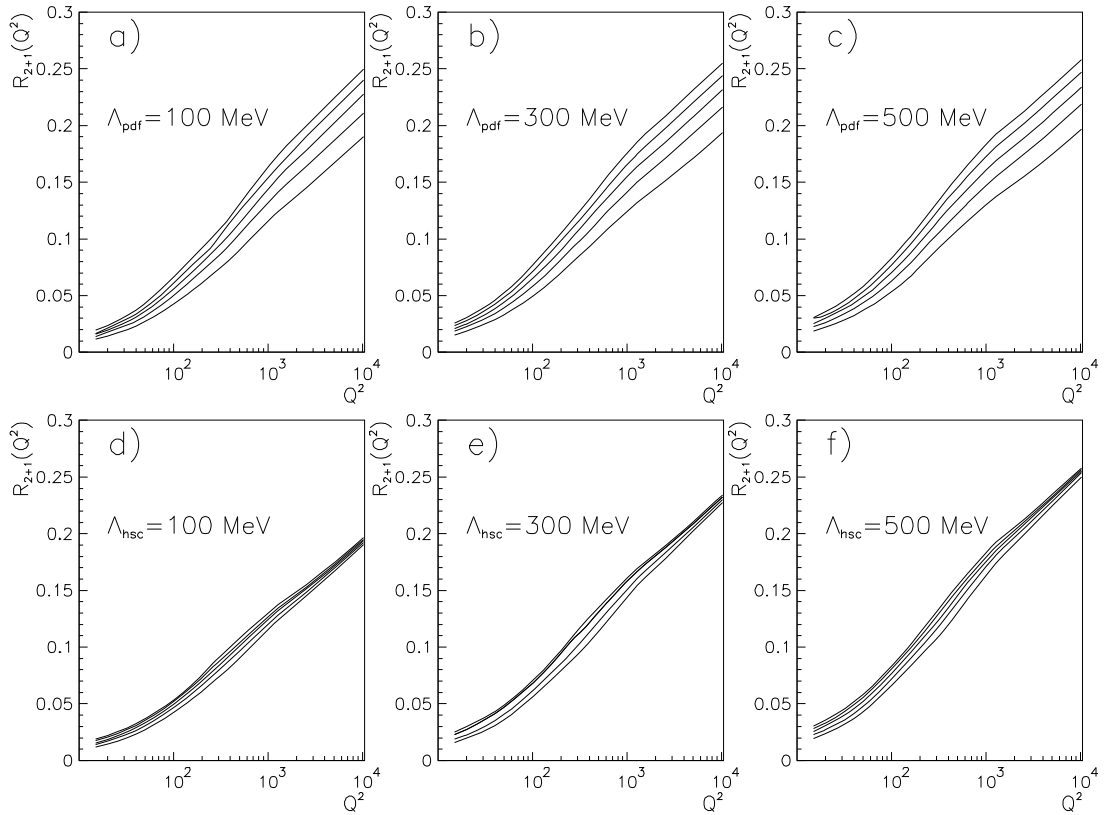


Figure 6: The same as in Fig. 3 but for the H1 acceptance cuts.

### 3.2 H1 cuts

In [1] only events satisfying certain acceptance cuts, most notably the cut on polar angle of outgoing jets in HERA laboratory frame,  $10^\circ \leq \theta_{\text{lab}}^{\text{jet}} \leq 145^\circ$ , were selected for the analysis. In Fig. 6 plots analogous to those of Fig. 3, but incorporating these cuts, are displayed. We see that the experimental cuts affect mostly the low  $Q^2$  region, where beside lowering the values of  $R_{2+1}(Q^2)$  they also strongly suppress the sensitivity of  $R_{2+1}(Q^2)$  to the variation of  $\Lambda$  in the PDF. This effect can be understood as follows. By imposing the mentioned angular cuts, one removes events with jets that fly into a large part of the backward (with respect to the proton direction) lab frame hemisphere. We recall that in direct photon interactions (in contrast to the resolved ones), i.e. also DIS, a large fraction of jets populates the backward hemisphere in the  $\gamma p$  CMS. Because the transverse boost between the  $\gamma p$  CMS and HERA lab frame is proportional to  $Q^2$ , the cut on the jet polar angle in the lab system is more effective for small  $Q^2$  than for high  $Q^2$ . Hence the drastic suppression of  $R_{2+1}(Q^2)$  at low and only moderate at high  $Q^2$ . Furthermore, as low  $Q^2$  means in average also small  $x$ , and most of the sensitivity of  $R_{2+1}(Q^2)$  to  $\Lambda$  in PDF comes from the small  $x$  region, the H1 cuts will significantly reduce it mainly for low  $Q^2$ .

On the basis of Fig. 6 we conclude that in the region  $Q^2 \geq 100 \text{ GeV}^2$ , used in [1] for the extraction of  $\Lambda$  from the measured  $R_{2+1}(Q^2)$ , the variation of  $\Lambda$  in the PDF could be neglected

with respect to the variation of  $\Lambda$  in the hard scattering cross-sections.

## 4 Conclusions

In this paper we have constructed parameterizations of PDF corresponding to solutions of the evolution equations with fixed suitably defined boundary conditions and variable  $\Lambda$ . These parameterizations were then used to investigate, for the quantity  $R_{2+1}$ , the numerical importance of varying  $\Lambda$  in PDF. We concluded that:

- If no cuts are applied on produced jets the sensitivity of (1) to variation of  $\Lambda$  in PDF is bigger at the LO than at the NLO.
- At moderate  $Q^2$ , roughly below 40 GeV<sup>2</sup>, the sensitivity of (1) to  $\alpha_s$  comes dominantly from PDF, while at higher  $Q^2$  the hard scattering cross-sections take rapidly over as the main source of the  $\Lambda$ -dependence of (1).
- The preceding conclusions are only weakly dependent on  $y_c$ .
- Including the cuts applied by the H1 Collaboration leads to strong suppression of the sensitivity to  $\alpha_s$  in the moderate  $Q^2$  region.

It is clear that a less restrictive treatment of the jets in the  $Q^2$  region between, say, 10 and 100 GeV<sup>2</sup> could provide much better possibility for a precise determination of  $\alpha_s$ . This region is also very interesting from another point of view, and namely the question of the transition between the dynamics of deep inelastic scattering and photoproduction. The data in this region could bring new information on the structure of the virtual photon [16] and/or lead to new phenomena.

## Acknowledgments

This work had been supported in part by the grant No. 201/96/1616 of the Grant Agency of the Czech Republic.

## References

- [1] T. Ahmed et al., H1 Coll.: Phys. Lett. **B 346** (1995) 415.
- [2] M. Derrick et al., ZEUS Coll.: Phys. Lett. **B363** 201.
- [3] D. Graudenz: PROJET 4.1 MC generator, CERN-TH.7420/94.
- [4] E. Mirkes, D. Zeppenfeld: MEPJET MC generator, Phys. Lett. **B380** (1996) 105, hep-ph/9511448
- [5] T. Brodtkorb, E. Mirkes: DISJET MC generator: Z. Phys. **C66** (1995) 141
- [6] D. Graudenz: Phys. Lett. **B 256** (1991) 518.
- [7] A.D. Martin, R.G. Roberts and W.J. Stirling: Phys. Rev. **D 47** (1993) 867.
- [8] J. Botts et al., CTEQ Coll.: Phys. Lett. **B 304** (1993) 159.
- [9] M. Glück, E. Reya, A. Vogt: Z. Phys. **C 67** (1995) 433.
- [10] J. Chýla, J. Rameš: PRA-HEP/96-01, hep-ph/9604306

- [11] H.D. Politzer: Nucl. Phys. **B 192** (1982) 493.
- [12] A. Buras: Rev. Mod. Phys. **52** (1980) 199.
- [13] M. Glück, E. Reya, A. Vogt: Z. Phys. **C 53** (1992) 127.
- [14] A. Vogt: Phys. Lett. **B 354** (1995) 145.
- [15] A. Martin, G. Roberts, W. J. Stirling: Phys. Lett. **356** (1995) 89.
- [16] J. Chýla, J. Cvach: in *Future Physics at Hera*, ed. G. Ingelman, A. de Roeck, R. Klanner, Hamburg 1996, p. 545